Morphology and Properties of PP/EPDM Binary Blends and PP/EPDM/Nano-$CaCO_3$ Ternary Blends

Lei Gong, Bo Yin, Lan-peng Li, Ming-bo Yang

College of Polymer Science and Engineering, State Key Laboratory of Polymer Materials Engineering, Sichuan University, Chengdu 610065, Sichuan, People's Republic of China

Received 2 September 2010; accepted 2 March 2011
DOI 10.1002/app.34536
Published online 28 July 2011 in Wiley Online Library (wileyonlinelibrary.com).

ABSTRACT: In this article, the morphology, crystallization, and rheological behaviors of polypropylene (PP)/ethylene-propylene-diene terpolymer (EPDM) binary blend and PP/EPDM/calcium carbonate nanoparticles (nano-$CaCO_3$) ternary blend were investigated. Two processing methods, i.e., direct extrusion and two-step extrusion, were employed to prepare the PP/EPDM/$CaCO_3$ blend. The influence of EPDM and nano-$CaCO_3$ respectively on phase morphology and properties of PP/EPDM blend and PP/EPDM/$CaCO_3$ blend were characterized by scanning electron microscopy (SEM), differential scanning calorimetry (DSC) and dynamic rheometer. The crystallinity and crystallization temperature of PP/EPDM blend were improved in comparison to pure PP due to addition of EPDM, but kept invariable with the increased EPDM loading. As the EPDM content was increased, the mobility of PP molecular chains was weakened. Compared with direct extruded blend, less and finer nano-$CaCO_3$ was dispersed in matrix of two-step extruded blend. Accordingly, the increased nano-$CaCO_3$ in matrix gave rise to a weaker increment in crystallinity and crystallization temperature of two-step extruded blend, and a later platform of tanδ curve. © 2011 Wiley Periodicals, Inc. J Appl Polym Sci 123: 510–519, 2012

Key words: morphology; properties; crystallization; rheology; polypropylene; EPDM; nano-particle

INTRODUCTION

It is well known that polypropylene (PP) is one of the important commodity polymers. It is extensively used in household appliance, automobile, and construction industry, due to its balanced mechanical properties. However, because of its brittleness at low temperature, high crystallinity, etc., the application of PP is restricted.[1–4] In past several decades, many methods have been taken to modify the toughness of PP.[5–7] Blending with elastomer is one of the effective methods to toughen PP, but at sacrifice of the strength of PP.[6,8–11] To reach a perfect balance of toughness and strength, the ternary polymer blends of PP/elastomer/nano-particles were developed. Nano-particles, such as nano-SiO_2,[3] short fibers[8] and nano-$CaCO_3$[12] were added to PP/elastomer system in order to achieve a simultaneous effective enhancement of toughness and strength of PP.

The phase morphology of this ternary polymer system, including elastomer and filler's distribution, core-cell morphology, the interfacial morphology and so on, was one of the crucial factors to influence the final mechanical properties[1,12,13] Morphology of the blends was influenced by several factors. Several researches[1,3,13–18] found that the final morphology of the ternary blends is determined by both thermodynamic and kinetic factors, such as interfacial tension, contact angle, viscosity ratio, composition, processing method, processing parameters, etc. Ma et al.[1] and Yang et al.[13] respectively predict dispersion state of nano-particles by calculating the wetting coefficient (ω_α), interfacial tension (γ_{AB}), and work of adhesion (W_{AB}). Premphet and Horanont[17] found that the phase structure of the composite was determined mainly by the chemical character of the components and, to a lesser degree, by the mixing sequences of each component. Wang et al.[15] discovered that the morphology of the ethylene-propylene-diene terpolymer (EPDM) particles were markedly influenced by the compounding route, whereas the dispersion degree of nano-$CaCO_3$ in the matrix was little influenced.

The properties of ternary systems, such as the crystallization and rheological properties, are remarkable dependent on its microstructure and morphology.[8,19–22] For example, the loss factor, tanδ (G''/G'), quantifies the balance of the loss and elastic properties and also provided an important information about the viscoelasticity of the nano-composites. The addition of elastomer and nano-particles had an effect on the crystal structure of the PP matrix, and a

Correspondence to: M.-B. Yang (yangmb@scu.edu.cn) or B. Yin (yinbo@scu.edu.cn).

Contract grant sponsor: National Natural Science Foundation commission of China; contract grant number: 20874066 and 50903050.

TABLE I
The Materials Used for the Preparation of Nano-$CaCO_3$ Suspension, PP/EPDM Blends and PP/EPDM/Nano-$CaCO_3$ Blends

Materials	Brand	Supplier	Characteristics
PP	T30s	Lanzhou Petrochemical Company, China.	MFR = 2.6 g/10 min Density = 0.91 g/cm^3
EPDM	4725P	Dupont Dow Elastomers L.L.C.	Containing 70% ethylene and 4.9% Ethylidene norbornene (ENB) M_w = 135,000 g/mol
Nano-$CaCO_3$	NPCC-201	Huaxin Nanomaterial	Particle size: 10–40nm
HPMC	HG-400	Tianpu Subtle Chemical Eng	

little change in the crystal structure of PP will lead to a change of property.[2] However, the effect of additives on the crystallization of PP is complicated due to the sensitivity of the morphology of PP to the temperature. These properties can always provide a good proof in polymer processing and in morphological characters, for they are sensitive to the particle size, shape, dispersion, and surface characteristics of the dispersed phase. So charactering the properties of ternary blends is useful to react the internal microstructure of these systems. Lee et al.[21] established the relationship between the rheology of the PP/LCP/nano-SiO_2 composites and the mixing sequence, the filler size, and the filler surface nature. The research team of Qiang Fu[19] assessed the deep mixing and morphology evolution of polymer composite with mixing time by rheological method.

However, few attentions have been paid to the effect of the addition and content of nano-$CaCO_3$ particles on the properties of PP/EPDM system, especially to the relationship between distribution of nano-$CaCO_3$ particles with mixing method and crystallization, rheological property of PP/EPDM/nano-$CaCO_3$ blends.

The main goal of this work is to study the crystallization and dynamic rheological properties of PP/EPDM binary blend and PP/EPDM/nano-$CaCO_3$ ternary blend. The morphological/mechanical behavior relationship of the ternary blend is also investigated. Two processing methods (direct extrusion and two-step extrusion) were used to prepare PP/EPDM/$CaCO_3$ ternary blends. Then, the influence of EPDM or nano-$CaCO_3$ particles content on the morphology and crystallization, dynamic rheological property of these blends are evaluated.

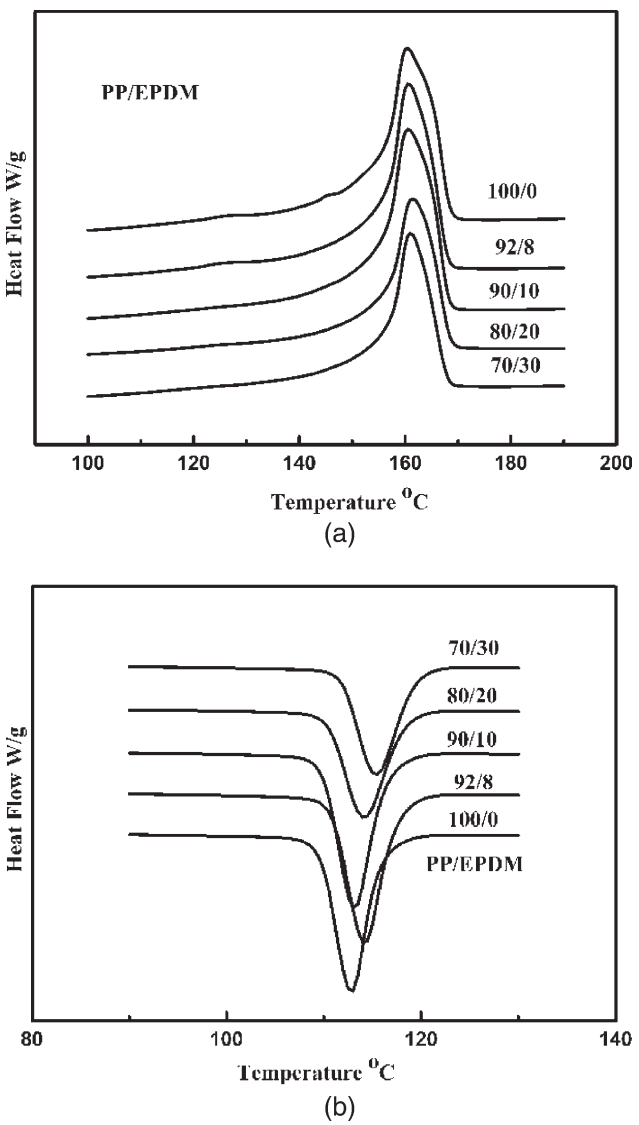

Figure 1 Melting (a) and nonisothermal crystallization (b) curves of pure PP and PP/EPDM blends.

TABLE II
Melting and Crystallization Parameters of Pure PP and PP/EPDM Blends

PP/EPDM	T_m (°C)	ΔH_c (J/g)	X_c (%)	T_c (°C)
100/0	160.4	73.04	35	112.83
92/8	160.61	72.87	38	114.23
90/10	160.52	76.28	41	113.15
80/20	161.46	60.3	36	114.16
70/30	161.04	58.02	40	115.4

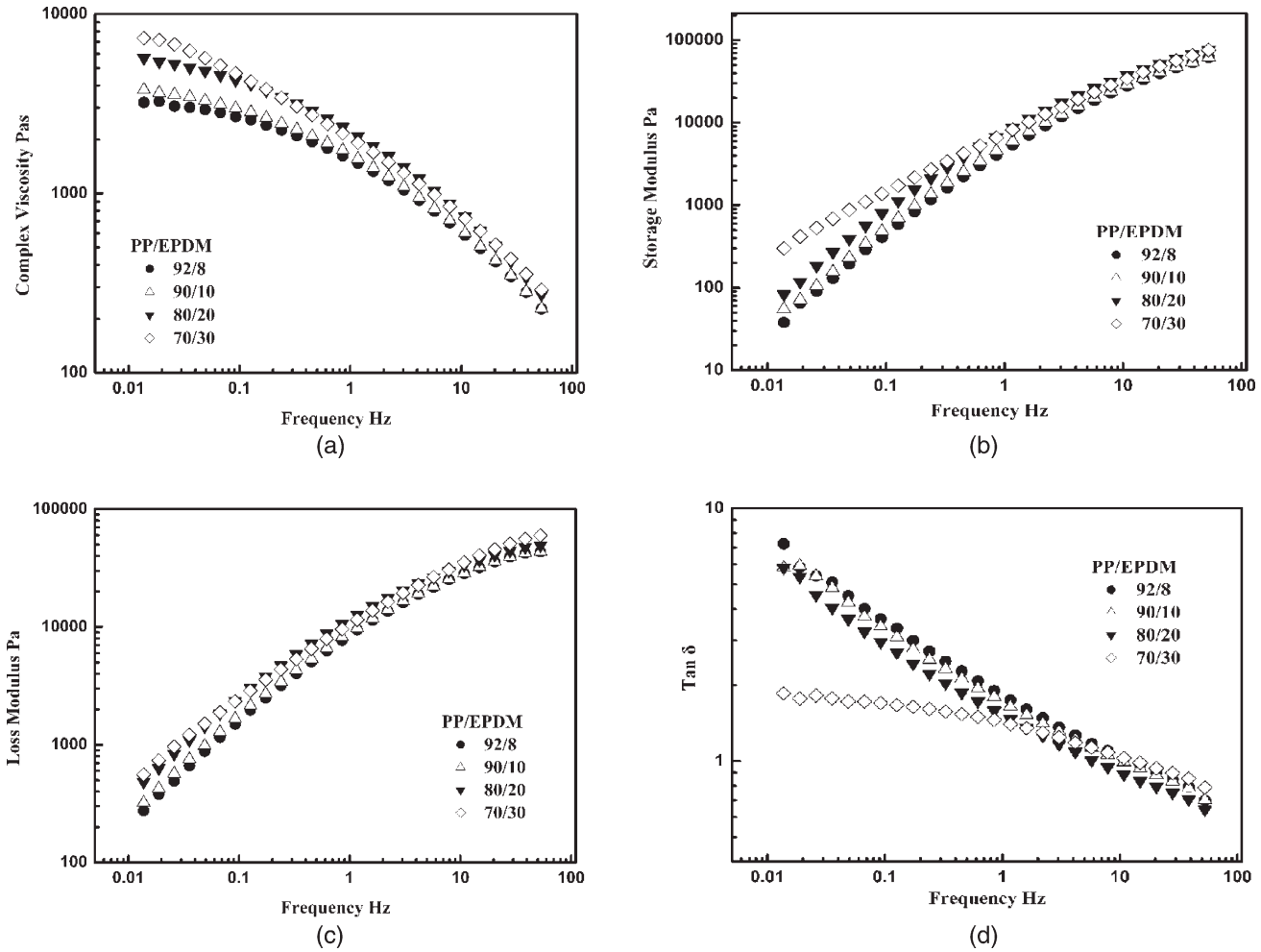

Figure 2 Angular frequency dependence of dynamic viscoelastic parameters for PP/EPDM blends at 200°C: (a) complex viscosity; (b) storage modulus; (c) loss modulus; and (d) loss factor.

EXPERIMENTAL

Materials

The materials used for preparation of nano-$CaCO_3$ suspension, PP/EPDM blends and PP/EPDM/nano-$CaCO_3$ blends are listed in Table I. PP, EPDM, nano-$CaCO_3$ particles and hydroxypropyl methylcellulose used in this study are commercially available. The nano-$CaCO_3$ particles were treated by stearic acid before trade.

Sample preparation

PP/EPDM binary blends were prepared by direct extrusion, whereas two processing methods were used to prepare PP/EPDM/$CaCO_3$ ternary blends. One is the direct extrusion, and the other is called two-step extrusion. In the direct extrusion, PP, EPDM, and nano-$CaCO_3$ were mixed in a CTE35 co-rotating twin-screw extruder (KEYA company, China) with a length/diameter ratio of 40 and a screw diameter of 35.6 mm. The extruding temperature was 200°C and the rotational speed was 100 rpm. In two-step extrusion, nano-$CaCO_3$ was suspended in a dispersant medium first, and then dispersed in EPDM using mild blending[23,24] method by means of a twin-screw extruder. The product was considered as pre-extrudate, and melt-blended with pure PP in the same twin-screw extruder and processing conditions as direct extrusion.

Scanning electron microscopic

The morphology of the blends was observed by preferential etching of EPDM phase in dimethylbenzene for 2 h. The samples were cryogenically fractured in the direction perpendicular to flow direction in liquid nitrogen before etching. The etched samples were carefully washed three times by using fresh dimethylbenzene, and then with acetone for three times. The samples were dried under air at room temperature for 24 h. The morphology of the

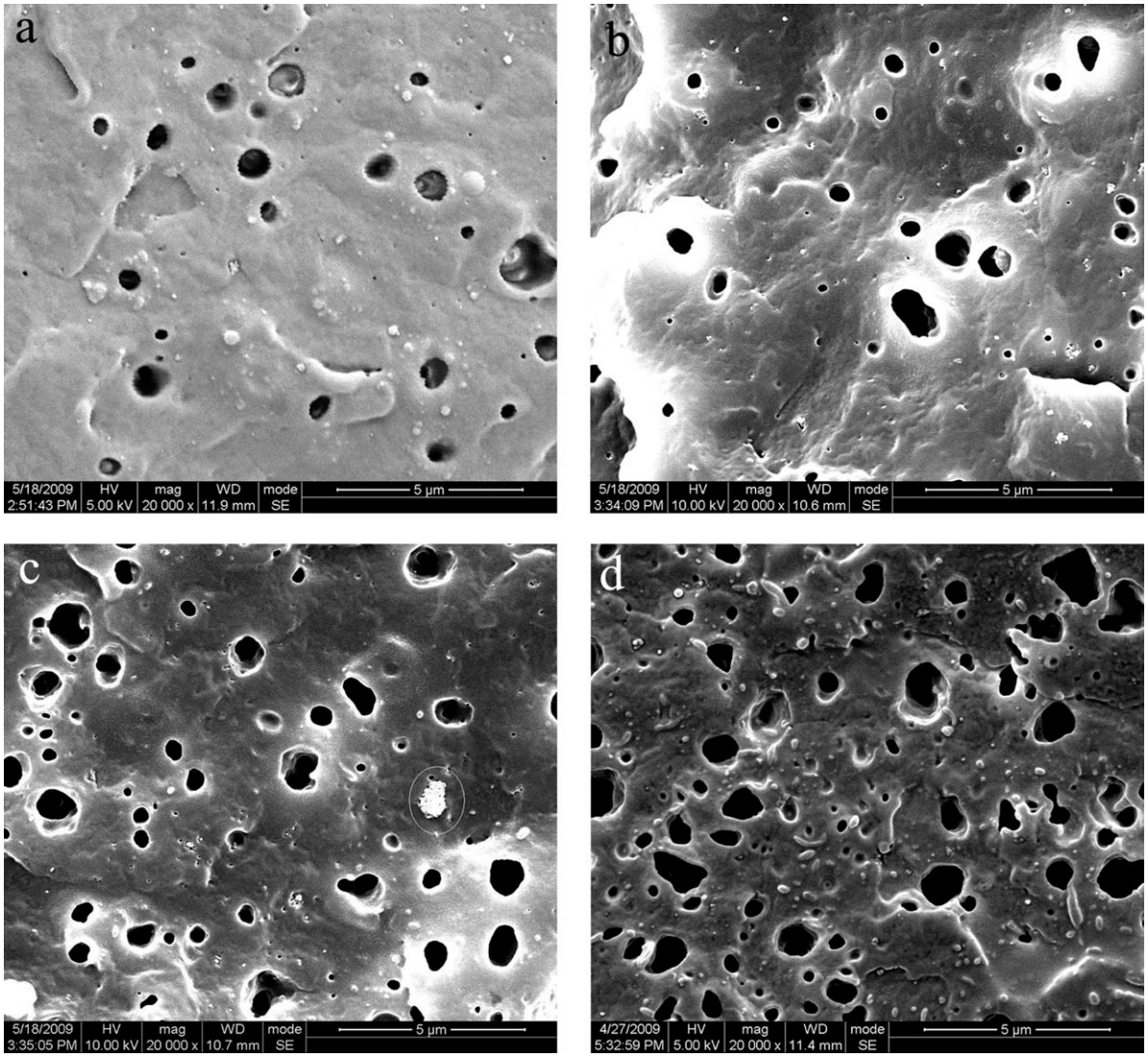

Figure 3 Phase morphology of PP/EPDM/$CaCO_3$ ternary blends prepared by direct extrusion with different composition (a) 92/8/0.8; (b) 90/10/1; (c) 80/20/2; and (d) 70/30/3.

fractured surface was observed by a JSM-5900LV SEM (scanning electron microscopy) instrument, using an acceleration voltage of 5 or 10 kV.

Differential scanning calorimeter

Thermal analysis measurements were performed using a TA Q20 differential scanning calorimetry (DSC). The sample of about 5 mg were quickly heated to 200°C and kept the temperature for 5 min to eliminate any thermal history in the material. Crystallization test was carried out in dynamic condition at a cooling rate of 10°C/min from 200 to 40°C, and melting test was carried out in dynamic condition at a heating rate of 10°C/min from 40 to 200°C. To confirm the thermal properties of the blends, at least three samples for each concentration were prepared and tested.

Dynamic rheology test

The materials were characterized using a Gemini 200 rheometer (Malvern) under a constant nitrogen flow. Measurements were performed in the plate-plate configuration with a gap of 1.20 mm in the frequency range from 0.01 to 100 Hz at 200°C.

RESULTS AND DISCUSSION

The properties of PP/EPDM binary blends

The melting and crystallization curves of pure PP and PP/EPDM blends are shown in Figure 1. All PP/EPDM blends showed a similar melting temperatures as pure PP at about 160°C as shown in Table II, illustrating the addition of EPDM has little influence on melting process and crystal perfection.

Crystallinity of PP was evaluated by the ratio between the enthalpy of fusion of the blend and the enthalpy of fusion of the perfectly crystalline PP ($\Delta H_{PP} = 209$ J/g).[25] It was observed that the crystallinity and crystallization temperature of PP were increased after addition of EPDM compared to pure PP however fluctuated with the increased EPDM loading, which indicated that EPDM could provide substantive nucleus.[8] The crystallinity of PP/EPDM blends reached its maximum at 10 wt % EPDM, whereas the highest crystallization temperature was achieved at 30 wt % EPDM.

The linear viscoelastic behavior of PP/EPDM blends is illustrated in Figure 2. The dynamic frequency sweep measurements were conducted at 200°C, and a strain of 1%. Naturally, with the increasing of the frequency, complex viscosities (η*) and loss factor (tanδ) are decreased, but storage modulus (G′) and loss modulus (G″) of PP/EPDM blends are increased. Complex viscosities (η*), storage modulus (G′), and loss moduli (G″) of the blend all increase monotonically with the EPDM content, especially at low frequency. All the samples exhibiting strong composition dependence are related to the high molecular weight and long molecular chains of EPDM, causing the mobility of EPDM is lower than that of PP molecular chains.

Loss factor (tanδ) decreasing with the increasing of EPDM content is shown in Figure 2(d), especially at low frequency. Surprisingly, a platform appeares in tanδ curve of the blend with 30 wt % EPDM, instead of a sustained reduction with frequencies. Such pseudo solid-like behavior[26,27] is probably attributed to a strong restriction of PP chains movement by the entanglement in EPDM chains.

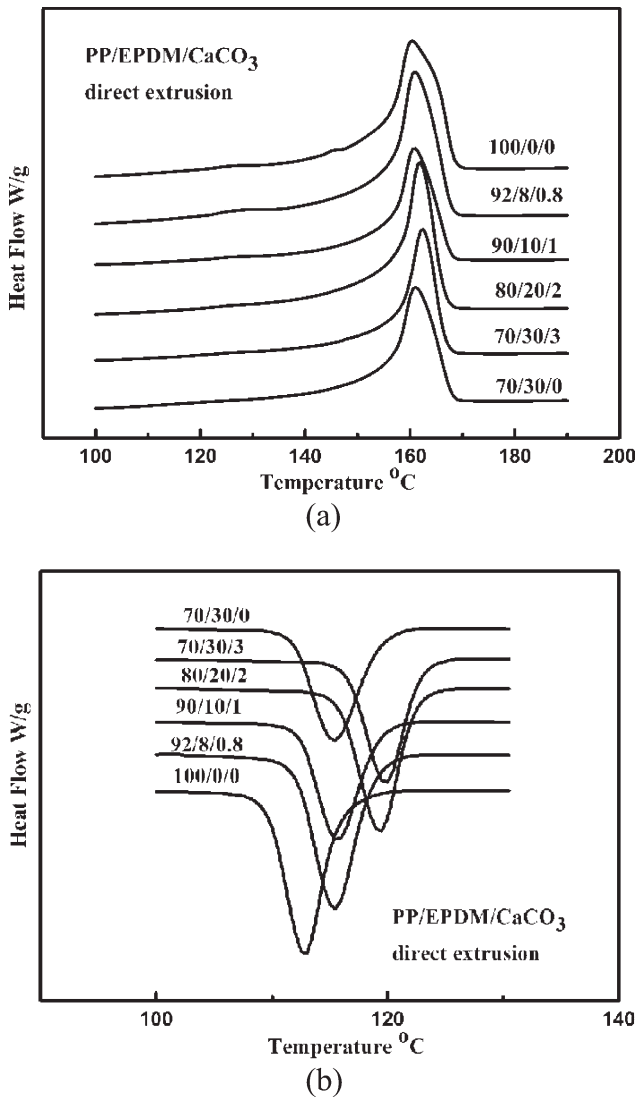

Figure 4 Melting (a) and nonisothermal crystallization (b) curves of PP/EPDM/$CaCO_3$ blends prepared by direct extrusion.

Morphology and properties of PP/EPDM/nano-$CaCO_3$ ternary blends prepared by direct extrusion

SEM micrographs of cryogenically fractured surfaces of direct-extrusion specimens of PP/EPDM/nano-$CaCO_3$ blends are demonstrated in Figure 3. The dark holes in the micrographs represent the etched EPDM phase and the white particles are nano-$CaCO_3$ particles. The interface between EPDM phase and PP phase is smooth. As the EPDM content increases, EPDM particles become larger and out of regularity.

Separated dispersion structure of PP/EPDM/nano-$CaCO_3$ blend prepared by direct extrusion is most likely formed as abundant nano-$CaCO_3$ particles are observed in PP phase. The quantity of nano-$CaCO_3$ particles in PP matrix increases with the increment of the nano-$CaCO_3$ content. Nano-$CaCO_3$ agglomerate shown in Figure 3(c) indicates nano-$CaCO_3$ is poorly dispersed in the matrix of this direct extruded blend when the nano-$CaCO_3$ content reaches about 2 wt %.

The melting and crystallization curves of PP/EPDM/nano-$CaCO_3$ blends prepared by direct extrusion are shown in Figure 4. A rise of melting temperatures of PP was demonstrated in Figure 4(a), indicative of an improvement of PP crystal perfection caused by the addition of nano-$CaCO_3$ into PP/EPDM blend. And a slight rise trend of PP melting temperatures in direct extruded blend was present with the increasing of nano-$CaCO_3$ content.

Table III shows the crystallinity of PP in PP/EPDM/nano-$CaCO_3$ blends obtained by direct extrusion. The crystallinity of PP in direct extruded ternary blends was higher than that of pure PP, and no obvious variation was observed with the increasing nano-$CaCO_3$ content, which showed a similar result

TABLE III
Melting and Crystallization Parameters of Direct-Extrusion PP/EPDM/$CaCO_3$ Blends

PP/EPDM/$CaCO_3$	T_m (°C)	ΔH_c (J/g)	X_c (%)	T_c (°C)
100/0/0	160.4	73.04	35	112.83
92/8/0.8	160.95	70.87	37	115.43
90/10/1	161.14	73.42	39	115.77
80/20/2	161.85	64.68	39	119.32
70/30/3	162.35	51.68	36	119.79
70/30	161.04	58.02	40	115.4

as PP/EPDM blends. It meant that the addition of nano-$CaCO_3$ had no influence on PP crystallinity.

Because of the heterogeneous nucleation effect of nano-$CaCO_3$, a pronounced improvement of onset crystallization temperatures of PP in PP/EPDM/nano-$CaCO_3$ blends than that in PP/EPDM blend is brought out. The onset crystallization temperature of PP in PP/EPDM/nano-$CaCO_3$ blends is increased along with the increased nano-$CaCO_3$ content, which is ascribed to the increased heterogeneous nuclei provided by nano-$CaCO_3$ in PP matrix.

The influence of nano-$CaCO_3$ content on the dynamic viscoelastic parameters of PP/EPDM/nano-$CaCO_3$ blends prepared by direct extrusion is revealed in Figure 5. The same as PP/EPDM blends, the complex viscosity and loss factor of direct extruded PP/EPDM/nano-$CaCO_3$ blends are decreased, whereas the storage modulus and loss modulus of these blends are increased with the increase of the frequency.

There is no obvious variation in the value of η^* and G'' of PP/EPDM/nano-$CaCO_3$ blends prepared by direct extrusion when nano-$CaCO_3$ content was low (less than 2 wt %). The result was much different from that of PP/EPDM blends, due to the involving of nano-$CaCO_3$ into the blends. Thus, a few nano-$CaCO_3$ particles dispersed in PP phase are helpful to the mobility of PP chains, which can weaken the resistance of EPDM chains is discussed

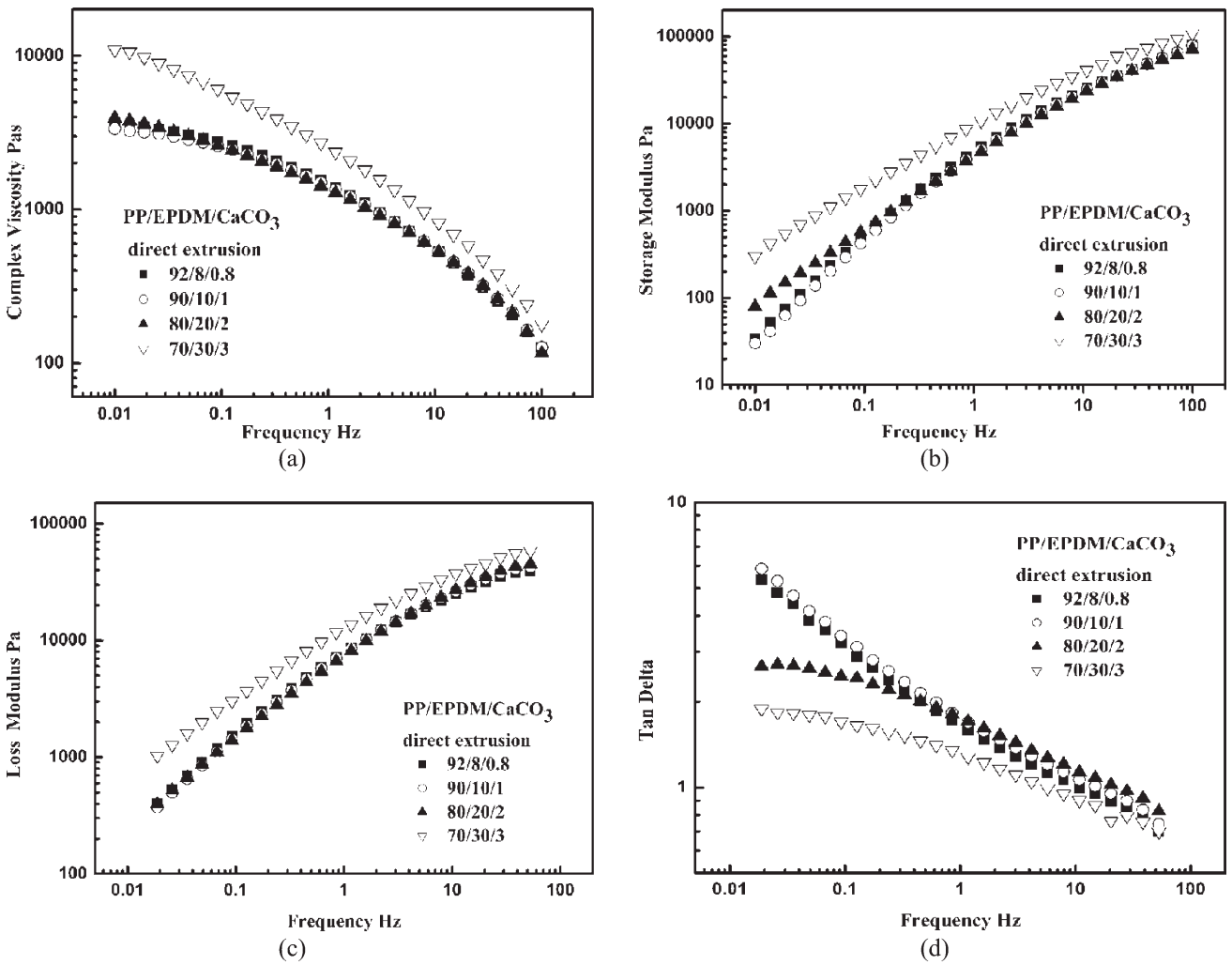

Figure 5 Angular frequency dependence of dynamic viscoelastic parameters for PP/EPDM/$CaCO_3$ blends prepared by direct extrusion: (a) complex viscosity; (b) storage modulus; (c) loss modulus; and (d) loss factor.

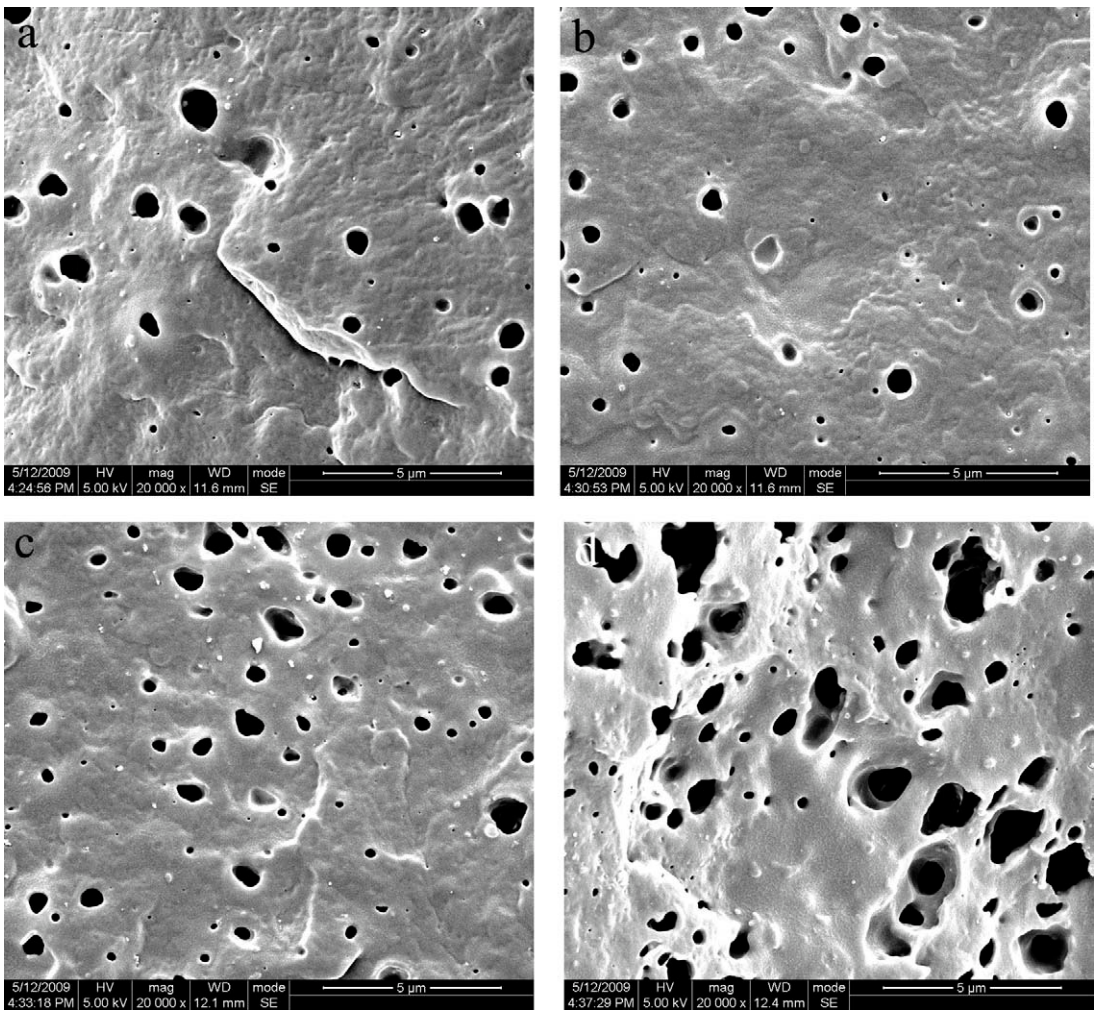

Figure 6 Phase morphology of PP/EPDM/nano-$CaCO_3$ ternary blends prepared by two-step extrusion with different composition (a) 92/8/0.8; (b) 90/10/1; (c) 80/20/2; and (d) 70/30/3.

above. However, a remarkable increment in both η* and G″ of the blends (PP/EPDM/nano-$CaCO_3$ 70/30/3) surprisingly appears. It is implied that when the nano-$CaCO_3$ content in PP phase reached a certain value, these particles would restrict the mobility of the PP chains. The variation of both η* and G″ of the direct extruded blend is due to the influence of $CaCO_3$ particles on the mobility of PP chains, which further confirms the existence of $CaCO_3$ particles in PP matrix. And the variation degree is related to the quantity of $CaCO_3$ particles dispersed in PP matrix.

The storage modulus (G′) of the PP/EPDM/nano-$CaCO_3$ blends obtained by direct extrusion also shows strong composition dependence, which was similar to PP/EPDM blends, especially at low frequency.

The tanδ of the PP/EPDM/nano-$CaCO_3$ blends prepared by direct extrusion is shown in Figure 5(d). The tanδ of the blends decreases with the increase of nano-$CaCO_3$ content. It is noteworthy that when the content of nano-$CaCO_3$ reaches 2 wt %, a platform is observed in tanδ curves at low frequencies, instead of a sustained reduction with the increasing frequencies. The platform emerges at the 20 wt % EPDM of PP/EPDM/nano-$CaCO_3$ blends prepared by direct extrusion, earlier than that of PP/EPDM blends, which is mostly attributed to the development of nano-$CaCO_3$ clusters in the PP phase that has been observed in SEM photos of direct extruded blends (Fig. 3).[26]

Morphology and properties of PP/EPDM/nano-$CaCO_3$ ternary blends prepared by two-step extrusion

The morphology of cryogenically fractured surfaces of PP/EPDM/nano-$CaCO_3$ ternary blends prepared by two-step extrusion is illustrated in Figure 6. Dark holes and white particles represent etched EPDM phase and nano-$CaCO_3$ particles, respectively. The EPDM distribution with the increasing of nano-$CaCO_3$ content in two-step extruded blends is

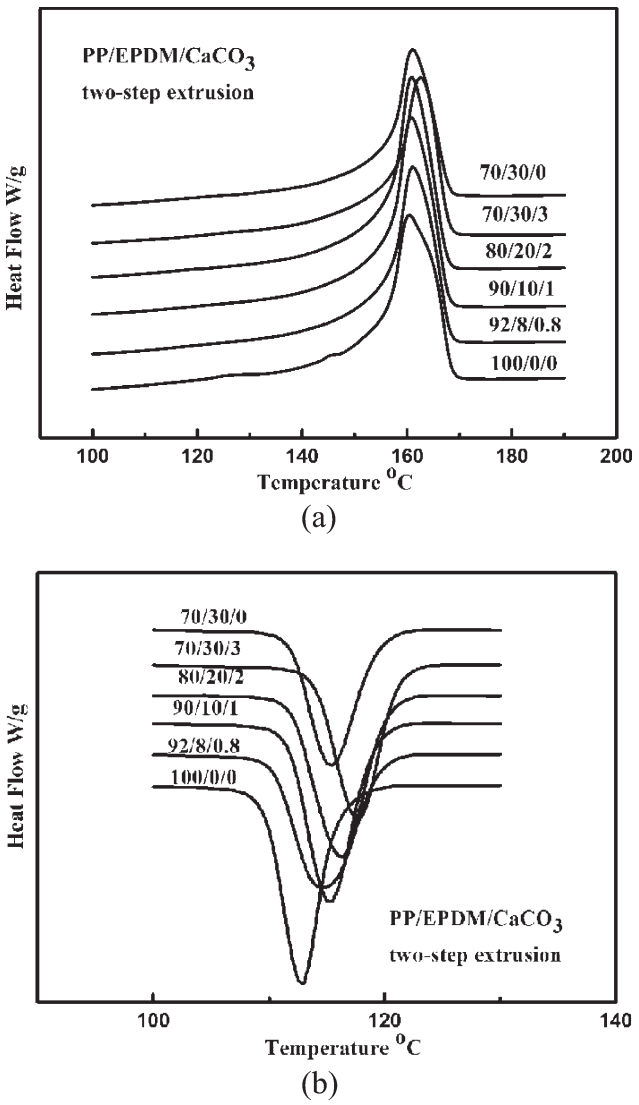

Figure 7 Melting (a) and nonisothermal crystallization (b) curves of PP/EPDM/$CaCO_3$ blends prepared by two-step extrusion.

similar to that in direct extruded blends. However, in comparison with counterparts prepared by direct extrusion, less nano-$CaCO_3$ particles in PP matrix was observed in ternary blends prepared by two-step extrusion, and the quantity of nano-$CaCO_3$ particles located in PP phase was lower with the increasing of nano-$CaCO_3$ content, compared with the corresponding ternary blends prepared by direct extrusion. Some nano-$CaCO_3$ particles are remained in EPDM phase by two-step extrusion, different from majority dispersing in PP phase by direct extrusion, though the migration of nano-$CaCO_3$ from EPDM phase to matrix occurred spontaneously under the drive of thermodynamics during the processing of two-step extrusion.

The melting and crystallization curves of PP/EPDM/nano-$CaCO_3$ blends prepared by two-step extrusion are displayed in Figure 7. No substantial differences in melting temperature of PP for two-step extruded blends are observed, which is similar to the result of PP/EPDM blends. Crystallinity of PP in PP/EPDM/nano-$CaCO_3$ blends prepared by two-step extrusion listed in Table IV, is larger than that of pure PP, and increases with the increase of nano-$CaCO_3$ content. It seems that the addition of nano-$CaCO_3$ has more effect on crystallinity of PP in the two-step extruded blends than in direct extruded blends.

The crystallization behavior of PP/EPDM/nano-$CaCO_3$ blends prepared by two-step extrusion is shown in Figure 7b. The increment in crystallization temperatures of PP in two-step extruded blends with the increase of nano-$CaCO_3$ content is slower and weaker, compared to direct extruded blends. For instance, when the nano-$CaCO_3$ content is 2 wt %, the crystallinity temperature of two-step extruded blends is about 3.5°C higher than pure PP, whereas that of direct extruded blends is over 7°C. It indicates that the heterogeneous nucleation effect of nano-$CaCO_3$ in two-step extruded blends is weaker than that in direct extruded blends, further implying that less nano-$CaCO_3$ particles existed in PP phase in two-step extruded blends than in direct extruded blends. Therefore, it can be concluded that the variation of crystallization temperatures is attributed to the different distribution of nano-$CaCO_3$ particles in PP phase caused by different processing methods.

The dynamic rheological parameters of PP/EPDM/nano-$CaCO_3$ blends prepared by two-step extrusion are displayed in Figure 8. The variation in the dynamic rheological parameters with frequency for the blends prepared by two-step extrusion is similar to the other two blends discussed above.

As shown in Figure 8, the η^*, G', and G'' of PP/EPDM/nano-$CaCO_3$ blends prepared by two-step extrusion increase with the increase of nano-$CaCO_3$ loading, whereas tanδ decreases with the increase of nano-$CaCO_3$ loading. A platform in tanδ curve at the low frequency does not appear until the nano-$CaCO_3$ content reaches its maximum, i.e., 3 wt %, which resembles the trend of PP/EPDM binary blends, but is different from that of direct extruded blends, indicative of a weaker influence of nano-

TABLE IV
Melting and Crystallization Parameters of PP/EPDM/$CaCO_3$ Blends Prepared by Two-Step Extrusion

PP/EPDM/$CaCO_3$	T_m (°C)	ΔH_c (J/g)	X_c (%)	T_c (°C)
100/0/0	160.4	73.04	35	112.83
92/8/0.8	161.02	72.34	38	114.69
90/10/1	160.75	75.61	41	115.28
80/20/2	160.84	73.77	45	116.24
70/30/3	162.6	62.22	44	117.69
70/30	161.04	58.02	40	115.4

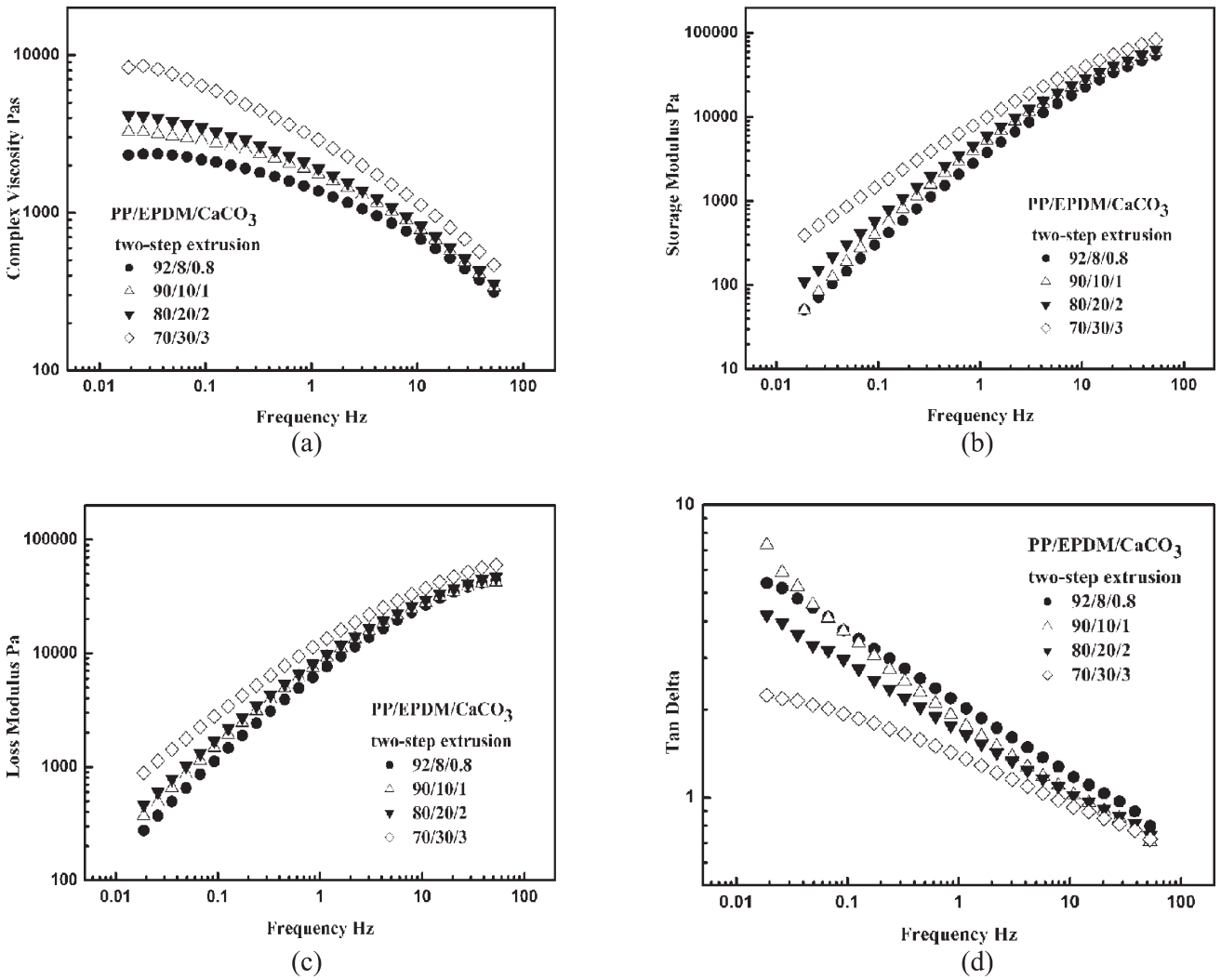

Figure 8 Angular frequency dependence of dynamic viscoelastic parameters for PP/EPDM/nano-$CaCO_3$ blends prepared by two-step extrusion: (a) complex viscosity; (b) storage modulus; (c) loss modulus; and (d) loss factor.

$CaCO_3$ on the mobility of PP chains in two-step extruded blends than in direct extruded blends. This phenomenon is related to the different distribution of nano-$CaCO_3$ particles brought by different processing methods. Therefore, in comparison with direct extruded blends, less nano-$CaCO_3$ particles are dispersed in PP phase in two-step extruded blends, in accordance with the results of SEM and DSC.

CONCLUSIONS

The morphology, crystalline property, and rheological behavior of PP/EPDM binary blends and PP/EPDM/nano-$CaCO_3$ ternary blends have been investigated. PP/EPDM/nano-$CaCO_3$ ternary blends were prepared by direct extrusion and two-step extrusion, respectively. The crystallinity and crystallization temperature of PP/EPDM blend were increased, compared with pure PP, due to addition of EPDM, but almost kept constant with the increasing EPDM loading. The crystallinity and crystallization temperature of PP in PP/EPDM/nano-$CaCO_3$ ternary blends further increased with the increasing nano-$CaCO_3$ content.

In PP/EPDM binary blends and PP/ EPDM/ nano-$CaCO_3$ ternary blends, EPDM could restrict the mobility of PP chains, due to the entanglement of EPDM chains, leading to the increase of complex viscosities, storage modulus and loss moduli. It is surprising that low nano-$CaCO_3$ particles loading (under 2 wt %) in PP phase were favorable for the movement of PP chains, i.e., weakening the resistance effect of EPDM chains on mobility of PP chains. However, abundant nano-$CaCO_3$ particles in PP phase would constrain the mobility of PP chains.

Separated dispersion structure was formed in PP/EPDM/nano-$CaCO_3$ blends prepared by direct extrusion, whereas less nano-$CaCO_3$ particles were dispersed in PP phase in ternary blends prepared by

two-step extrusion, which was responsible for a less increment in crystallinity and crystallization temperature of PP, and a later platform of tanδ in two-step extruded blend than that of in direct extruded blend.

References

1. Ma, C. G.; Zhang, M. Q.; Rong, M. Z. J Appl Polym Sci 2007, 103, 1578.
2. Da Silva, A. N.; Tavares, M. B.; Politano, D. P.; Coutinho, F. B.; Rocha, M. G. J Appl Polym Sci 1997, 66, 2005.
3. Yang, H.; Zhang, Q.; Guo, M. Polymer 2006, 47, 2106.
4. Frounchi, M.; Dadbin, S.; Salehpour, Z. J Membrane Sci 2006, 282, 142.
5. Liu, Z. H.; Zhang, X. D.; Zhu, X. G. Polymer 1997, 38, 5267.
6. van der Wal, A.; Mulder, J. J.; Oderkerk, J.; Gaymans, R. J. Polymer 1998, 39, 6781.
7. Inoue, T.; Suzuki, T. J Appl Polym Sci 1996, 59, 1443.
8. Arroyo, M.; Zitzumbo, R.; Avalos, F. Polymer 2000, 41, 6351.
9. Jain, A. K.; Nagpal, A. K.; Singhal, R. J Appl Polym Sci 2000, 78, 2089.
10. Jafari, S. H.; Gupia, A. K. J Appl Polym Sci 2000, 78, 962.
11. van der Wal, A.; Nijhof, R.; Gaymans, R. J. Polymer 1999, 40, 6031.
12. Ma, C. G.; Mai, Y. L.; Rong, M. Z. Compos Sci Technol 2007, 67, 2997.
13. Yang, H.; Zhang, X. Q.; Qu, C. Polymer 2007, 48, 860.
14. Wang, X.; Xu, K. J.; Xu, X. B. J Appl Polym Sci 2009, 113, 2485.
15. Wang, X.; Sun, J.; Huang, R. J Appl Polym Sci 2006, 99, 2268.
16. Fenouillot, F.; Cassagnau, P.; Majeste, J.-C. Polymer 2009, 50, 1333.
17. Premphet, K.; Horanont, P. Polymer 2000, 41, 9283.
18. Lee, H.; Fasulo, P. D.; Rodgers, W. R. Polymer 2005, 46, 11673.
19. Yang, H.; Li, B.; Wang, K. Eur Polym J 2008, 44, 113.
20. Aciemo, D.; Filippone, G.; Romeo, G. Macromol Symp 2007, 247, 59.
21. Lee, M. W.; Hu, X.; Li, L. Polym Int 2003, 52, 276.
22. Gu, S. Y.; Ren, J. J Polym Sci: Part B 2007, 45, 3189.
23. Li, W; Liu, Z. Y.; Yang, M. B. J Appl Polym Sci 2010, 115, 2629.
24. Tao, R.; Liu, Z. Y.; Yang, W.; Yang, M. B. Polym-Plast Technol 2008, 47, 490.
25. Valentini, L.; Biagiotti, J.; Kenny, J. M. J Appl Polym Sci 2003, 89, 2657.
26. Osman, M. A.; Atallah, A. Polymer 2005, 46, 9476.
27. Osman, M. A.; Atallah, A. Polymer 2006, 47, 2357.